Influence of fictive temperature and composition of silica glass on anomalous elastic behaviour

2006 J. Phys.: Condens. Matter 18 7507

(http://iopscience.iop.org/0953-8984/18/32/001)

J. Phys.: Condens. Matter **21** (2009) 079802 (1pp) doi:10.1088/0953-8984/21/7/079802

Corrigendum

Influence of fictive temperature and composition of silica glass on anomalous elastic behaviour
R Le Parc, C Levelut, J Pelous, V Martinez and B Champagnon 2006 *J. Phys.: Condens. Matter* **18** 7507–27

It has come to the attention of the authors that in the above article a small error has occured in the third paragraph of page 7511. The first sentence is corrected as follows:

As for the evolution of the density with OH content, a decrease by 0.96×10^{-6} for each 1 wt ppm of water regardless of T_F has been reported [43].

INSTITUTE OF PHYSICS PUBLISHING JOURNAL OF PHYSICS: CONDENSED MATTER

J. Phys.: Condens. Matter **18** (2006) 7507–7527 doi:10.1088/0953-8984/18/32/001

Influence of fictive temperature and composition of silica glass on anomalous elastic behaviour

R Le Parc[1], C Levelut[1], J Pelous[1], V Martinez[2] and B Champagnon[2]

[1] Laboratoire des Colloides, Verres et Nanomatériaux, CNRS/UMR5587, Université Montpellier II, cc 69, 34095 Montpellier Cedex, France
[2] Laboratoire de Physico-Chimie des Matériaux Luminescents, Université Lyon 1, CNRS/UMR 5620, 69622 Villeurbanne Cedex, France

E-mail: leparc@lcvn.univ-montp2.fr

Received 30 March 2006, in final form 12 June 2006
Published 25 July 2006
Online at stacks.iop.org/JPhysCM/18/7507

Abstract

In order to determine the influence of the thermal history (fictive temperature) and OH content on the elastic properties of silica glass, we have investigated high resolution *in situ* Brillouin experiments on SiO_2 glass from room temperature to the supercooled liquid at 1773 K across the glass transition. The well known anomalous increase of elastic modulus in the glassy state and in the supercooled liquid regime is observed. No change in the slope of the elastic moduli of silica appears as a characteristic of the glass transition, in contrast to what happens in various other glasses. We show that thermal history has a weak effect on elastic moduli in the glass transition regime for silica glass. The effect of the water content in silica glass is greater than the fictive temperature effect and gives larger changes in the amplitude of the elastic modulus for the same thermal dependence. A singular decrease above 1223 K is also observed in the shear moduli for hydrated samples. Different models explaining the temperature dependence of the elastic properties in relationship with frozen-in density fluctuations or with the structure are discussed.

1. Introduction

Silica glass is one of the most widely studied materials both theoretically and experimentally. On one hand silica glass is often considered as the archetype of an amorphous material. On the other hand some properties of silica glass behave anomalously with temperature: density, thermal expansion, internal friction and elastic moduli show different behaviours compared to crystals or other glasses [1]. Upon compression some anomalous variations are also reported for elastic properties: elastic moduli decrease from room pressure up to 2–3 GPa and increase for higher pressures [2].

1.1. Thermal dependence of the elastic properties

In this paper, our interest will be focused on the thermal variation of elastic properties in different silica glasses. For most glasses (alkali silicates, for example), elastic moduli decrease slightly in the glassy state and decrease with an important slope in the supercooled liquid state [3–5]. High temperature elastic moduli in silica have been measured by Brillouin light scattering [6–10] and ultrasonic measurements [11]. Both types of measurement have shown that elastic moduli increase with temperature, strongly in the glassy regime above 1000 K and slightly in the supercooled liquid regime. Another anomalous temperature variation has also been reported at low temperature: the elastic modulus is characterized by a minimum around 83 K [12] related to a broad acoustic loss peak [13, 14] also seen at hypersonic frequencies [15–17].

Several explanations either based on phenomenological approaches or on structural origins have been proposed for the anomalous elastic behaviour in silica.

Among phenomenological approaches, Anderson reported a possible link between elastic properties and the thermal expansion coefficient [18]. In silica glass, the thermal expansion coefficient presents two particularities: between absolute zero and room temperature, silica glass exhibits a negative thermal expansion coefficient α [1, 12] and at higher temperature, although positive, the thermal coefficient of silica glass is 10–30 times smaller than in alkali silicate glasses [12, 19]. Anderson postulates that the thermal dependence of the modulus can be considered as the sum of a pure volume term at constant temperature and a pure temperature term at constant volume. Thus the elastic moduli M can be expressed as a function of volume and temperature following equation (1):

$$\mathrm{d}M/\mathrm{d}T = \alpha V(\mathrm{d}M/\mathrm{d}V)_{\mathrm{T}} + (\mathrm{d}M/\mathrm{d}T)_{\mathrm{V}}. \tag{1}$$

First, the second term in the equation is positive. Secondly, the first term is very small for silica glass because of the small thermal expansion. Finally, the sum of the two terms in silica glass is positive. In a normal glass, as the thermal expansion is not small the first term is not negligible and gives rise to a negative $\mathrm{d}M/\mathrm{d}T$. This explanation is based on the idea that a positive temperature coefficient of the moduli would be expected every time α is small. However GeO_2 and BeF_2 glasses both have rather large thermal expansion coefficients although they show positive thermal dependences of the elastic moduli [12].

Several models giving an interpretation of the anomalous elastic moduli for silica glass based on elastic inhomogeneities [20] or on the coexistence of two different structural states [21, 1] will be discussed in the following.

1.2. Dependence of the elastic properties on impurities and thermal history

Measurements of elastic properties from the literature have been performed on silica glasses of different origin and have proved that silica glasses from different sources or with different thermal histories are characterized by different measurable properties [19].

The thermal history of a glass can be characterized by the fictive temperature T_{F}, a quantity introduced by Tool [22]. The fictive temperature is defined as the temperature at which the liquid structure is frozen when cooling down through the glass transition. In the glassy state T_{F} is constant and $\mathrm{d}T_{\mathrm{F}}/\mathrm{d}T = 0$. In the glass transition range $\mathrm{d}T_{\mathrm{F}}/\mathrm{d}T$ varies from 0 to 1 and in the equilibrium state $\mathrm{d}T_{\mathrm{F}}/\mathrm{d}T = 1$. The fictive temperature characteristic of a given sample can be changed by isothermal treatment at a temperature T_{a} in the glass transition range. During annealing at T_{a}, properties of the material are going to evolve with time, in order to reach the equilibrium corresponding to this temperature T_{a}. During the treatment, $\mathrm{d}T_{\mathrm{F}}/\mathrm{d}T$ slowly relaxes from 0 to 1. After a long enough treatment time τ_{a} the properties no longer evolve and

the sample is stabilized. The sample can then be quenched from T_a to room temperature in order to freeze the new equilibrium and to obtain a sample with $T_F = T_a$ provided the quenching rate is fast enough. When the temperature of the treatment is in the lower part of the glass transition interval, the relaxation process is usually described by the term 'ageing'.

The influence of thermal history on many properties of silica glass has been studied in various papers [19, 23–32]. Some properties have been found to behave anomalously compared to most other glasses. For example, when the fictive temperature is raised, the density and refractive index increase in silica glass [19, 23, 33] whereas they decrease in most usual silicate glasses [35].

Silica glasses are usually classified into four categories with regard to their synthesis process [19]. Class I silica glasses are produced from natural quartz by electric fusion under vacuum or under an inert gas atmosphere. They contain a few ppm OH but a high concentration of metallic impurities (Al or Na). Class II silica glasses are produced from crystalline quartz powder by flame fusion, thus the OH content is about 150–400 ppm but the content of metallic impurities is low. Types III and IV silica glasses are produced by hydrolysis of $SiCl_4$, they contain about 100 ppm of chlorine and about 1000 ppm of OH (class III) or 0.4 ppm OH (class IV). In this paper we will work on samples from classes I, III and IV and a sol–gel glass prepared from a heat treated aerogel.

Several papers [36–38] have pointed out several modifications of the properties of silica glass induced by aluminium, fluorine, chlorine and OH impurities. In this paper we will mainly concentrate on the influence of OH content measured for some properties in the literature [19]. The influence of OH content and fictive temperature are somewhat intricate: increasing OH concentration also induces a decrease in viscosity [39], and therefore the glass transition interval and/or fictive temperature are also modified by OH content.

The aim of this paper is to extend available data for silica glass using samples of various origins, thermal treatment and OH content. Acoustic properties will be deduced from *in situ* temperature Brillouin shift measurements performed from room temperature up to high temperatures, extending above the glass transformation range. Elastic moduli will be deduced taking into account the variations of many different parameters used for the calculation of moduli (refractive index, density, etc). We also want to focus on the influence of thermal history and of OH content on relaxation processes around T_g.

2. Experimental results

2.1. Experimental devices

Brillouin light scattering corresponds to coherent inelastic scattering associated with the interaction of light with long wavelength elastic waves (phonons) due to propagating thermal vibrations in condensed materials. It reflects the dynamics of the elastic excitations, which is determined through the viscoelastic properties of the scattering medium. Thus, Brillouin scattering gives access to the elastic properties at small wavevectors (compared to ultrasonic experiments) and at high frequencies (typically 30 GHz).

Brillouin scattering measurements of transverse and longitudinal sound velocities at hypersonic frequencies have been performed using a high resolution Fabry–Perot interferometer [40, 41]. The incident light was the 514.5 nm line of a single mode argon ion laser. The incident power of the laser was about 600 mW. A two- or four-pass plane Fabry–Perot, with a free spectral range equal to 75 or 56 GHz and finesse equal to 40 is used as the monochromator. The frequency corresponding to the maximum transmission of this filter is matched with the frequency of the Brillouin line. The resolving unit is a spherical Fabry–Perot

(SFP) interferometer with a free spectral range of 1.48 GHz and a finesse of 50. The total contrast is about 10^9. The measurements of the longitudinal Brillouin shifts in samples were performed in backscattering geometry in a Linkam TS1500 heating device designed to work from 335 to 1773 K. Transverse shifts were measured with a right angle geometry in a furnace with optical windows built by Hermann Moritz (maximum power 4 kW, maximum temperature 1773 K).

The Brillouin peak position is measured between two consecutive orders with the spherical Fabry–Perot (SFP) interferometer (figure 1) and thus the determination of the Brillouin shift includes an error in the determination of the peak position but also an error in the determination of the free spectral range of the SFP. The hypersound velocity $V_{L/T}$ (L for longitudinal and T for transverse sound velocity) can then be calculated from the Brillouin shift $\nu_{L/T}$, from the refractive index n at a wavelength $\lambda_0 = 514.5$ nm, and from the scattering angle ($\theta = 180°$ for backscattering) according to equation (2):

$$V_{L/T} = \Delta\nu_{L/T}\lambda_0/(2n\sin(\theta/2)). \tag{2}$$

Due to the aperture of the collecting lens, the broadening line is much more important for 90° angle geometry measurement (transverse shift measurements) than in the backscattering configuration (longitudinal shift measurements).

Considering all those source of error, the total uncertainty in the determination of sound velocity is about 5 m s^{-1} for longitudinal sound velocity (in the backscattering geometry) and about 30 m s^{-1} for transverse sound velocity (with 90° angle geometry). The error in the refractive index is discussed in section 2.2.

The longitudinal modulus M (or C_{11}) and the shear modulus G (or C_{44}) can be calculated from the longitudinal sound velocity and transverse sound velocity and sample density (equation (3) and (4)):

$$M = \rho V_L^2 \tag{3}$$

$$G = \rho V_T^2. \tag{4}$$

Brillouin scattering measurements correspond to very high frequencies, often considered as infinite frequencies compared to other determinations of mechanical properties. The adiabatic compressibility (at infinite frequency) β_∞ can be calculated from the inverse of the compression modulus K determined from Brillouin measurements (equation (5)):

$$K = M - 4/3G \qquad \text{and} \qquad 1/K = 1/(M - 4/3G) = \beta_\infty. \tag{5}$$

2.2. Parameters for the determination of elastic properties

Determinations of sample density and refractive index are necessary in order to deduce mechanical properties from Brillouin data (equations (2–4)). For this study variations in refractive index and density with fictive temperature and OH content have to be considered.

For the silica glass samples studied, containing a few ppb OH (presented in section 2.3), density has been measured using a pycnometer in toluene [42]. An increase in the density ρ by about 0.2% with T_F is observed in the interval 1373–1773 K. The general evolution can be roughly approximated to a linear law (equation (6)):

$$\rho = 10^{-5}T_F + 2.1869. \tag{6}$$

Data from the literature show that the density of silica glass increases with increasing fictive temperature in the range 1373–1673 K [19, 23, 43]. An increase in density (and thermal expansion) with quenching rate has also been observed using molecular dynamic simulation [44].

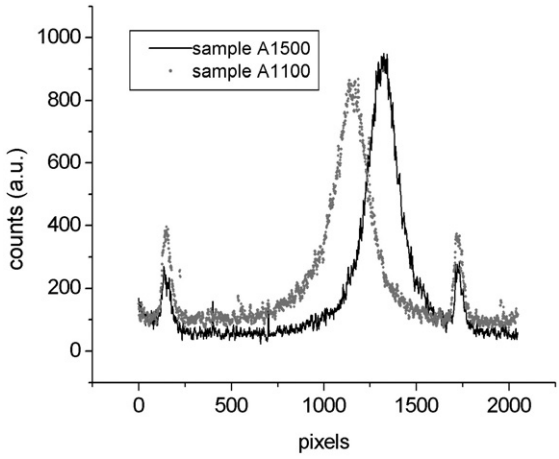

Figure 1. Spectra of Brillouin scattering at room temperature for sample A silica glasses, respectively heat treated at 1373 and 1773 K (table 1c). The two weak peaks correspond to elastic scattering of the incident laser at frequencies corresponding to two consecutive orders.

Data from Bruckner [19] show a maximum in the density for T_F in the range 1673–1773 K, but this result has been attributed to the impossibility of reaching high fictive temperatures with air or water quenching [45]. In the case of the samples studied, these have been proved to be well stabilized by other characterizations (Raman and IR) [46, 47]. The density difference between the samples heat treated at 1723 and 1773 K (table 1c) is within the experimental error, so it appears difficult to draw a conclusion about a potential maximum density for our samples. In a recent paper from Sen [48], a density minimum for a fictive temperature equal to 1223 K is reported for silica glass. Such a minimum has been observed for our samples around 1373 K [49], but the relaxation time at 1223 K in dehydrated samples containing a few ppm Al is very long and the stabilization of the samples (during 1 month of heat treatment) is to be verified.

The dependence of density on temperature can be estimated from the linear thermal expansion coefficient taken as equal to 0.5×10^{-6} K^{-1}. The volume thermal expansion $\Delta V/V = \Delta\rho/\rho$ is then equal to 1.5×10^{-6} K^{-1} and for $\rho = 2.203$, the density variation in the range of measurements, $\Delta\rho = 3.304 \times 10^{-6}$, can be neglected.

As for the evolution of the density with OH content, an increase by 0.96×10^{-6} for each 1 wt ppm of water regardless of T_F has been reported [42]. In a paper from Fraser [50] the increase in density for a constant fictive temperature is estimated to be 0.5×10^{-6}/wt ppm.

The refractive index versus fictive temperature $n(T_F)$ has been measured in different papers [19, 23, 33]. It increases almost linearly with increasing fictive temperature from 1273 to 1673 K and can be related to density variations, as shown in [23]. As for the density, above 1673 K the existence of a refractive index maximum is also debated. Different slopes can be found for $n(T_F)$, according to wavelength and silica glass composition. For the analysis of our data, we used for our samples an interpolation for $n(T_F)$ from values of the literature [19, 23] on silica glasses having the closest composition. Values are reported in table 1c.

A law for temperature dependence of the refractive index for silica glass has been suggested by Polian [10], from the comparison between Brillouin shift and ultrasonic measurements [11], but at high frequencies and low frequencies sound velocity can have different values if relaxation takes place. As in this work we want to study relaxation effects

Table 1a. Characteristics of the different commercial samples studied, their impurity content is given when known.

Sample	A	B	C	D	E	F
Origin	GE	Puropsil A Quartz et silice	Suprasil W Heraus	Sol–Gel	GE 124 fused quartz	Corning 7980
Class	I	I	IV		I	III
[OH]	ppb	20 ppm	0.4 ppm	3000 ppm	2 ppm	900 ppm
Other impurities	Al	Metallic	200 ppm Cl			Cl
Density	2.204	2.203	2.204	2.20		

Table 1b. Characteristics of the commercial samples studied by Fraser [50]. Our results will be compared to the results shown in his low frequency ultrasonic study.

Sample	Fraser [50]	Fraser [50]
Origin	IR Vitreosil	Corning 7940
Class	I	III
OH	2.4 ppm	900 ppm
Other impurities	—	Cl
Density	2.2024	2.2013

Table 1c. Characteristics of the heat treated samples A: densities measured by pycnometer and refractive index estimated from Bruckner [19] and [23] for samples having compositions close to that of sample A.

Sample A	AS	A1100	A1200	A1300	A1350	A1450	A1500
Annealing temperature	As received	1373 K	1473 K	1573 K	1623 K	1723 K	1773 K
Density (±0.001)	2.204	2.201	2.202	2.204	2.205	2.206	2.206
Refractive index (300 K, 514 nm)	1.4627	1.4624	1.4625	1.4626	1.4627	1.4628	1.4628

in the glass transition range, we use instead a thermal dependence of refractive index measured and presented by Bruckner [19] for a class II silica glass: $n(T)$ grows from 273 to 1273 K—almost linearly following equation (7):

$$n(T) = n(\text{room temperature}) + T \times 18.6 \times 10^{-6} + 0.6 \times 10^{-8} \times T^2 - 0.0002. \quad (7)$$

We have extrapolated this law for all the measured temperatures. No experimental measurement of the value of $n(T)$ above 1273 K reported in literature can verify the extrapolation, but the continuous evolution of $n(T)$ up to 2000 K shows adequate agreement with reference [10].

Haken reports slight modifications of the refractive index induced by OH, Cl and F impurities [33]. Actually, as OH groups in silica glass are expected to break some Si–O–Si bridges, the number of non-bridging oxygens (having a higher polarizability) is expected to increase when OH concentration increases; thus the refractive index is expected to increase slightly with increasing OH content. The refractive index is not always known with accuracy in the case of samples of a different nature found in the literature; then an error in the determination of the refractive index has to be considered. We used an error in the refractive index of $\Delta n = 5 \times 10^{-4}$, which leads to an additional estimated error of around 2 m s^{-1} for the sound velocity.

2.3. Samples

The first set of samples (table 1c) is composed of silica glasses A (class I) with a low OH content (some ppb) which have been heat treated at a temperatures T_a ranging from 1373 to 1773 K, and quenched fast enough in order to freeze-in the new structural organization. The

sample treatments have been detailed in a previous paper [46]. Apart from the heat treatment achieved at 1373 K over 6 days, all the samples have been heat treated for 1 h and 45 min. This treatment time, t_a, is longer than the stabilization time at those different temperatures. The structural evolution of the samples versus fictive temperature has been characterized by various experimental techniques [46, 47, 51].

A second set of samples (table 1a) containing silica glasses prepared by different methods was investigated. Two commercial samples have been widely studied: sample B, so-called 'Puropsil A', is a fused quartz provided by Quartz et Silice, produced from natural quartz by electrical fusion. Sample C, so-called 'Suprasil W' from Heraeus is synthetic silica produced from $SiCl_4$ in a water-free plasma flame. Two extra samples presented in [52] have also been measured at room temperature: sample E, so-called 'GE-124' from General Electrics, and sample F, so-called 'Corning 7980'. Finally sample D is a sol–gel silica, prepared using an aerogel of initial density 0.3 g cm^{-3}, heat-treated at about 1373 K for several hours until its density reaches the value 2.20 g cm^{-3} of amorphous silica. This sample corresponds to a higher OH content as well as a lower heat treatment temperature. The OH and impurity contents of the samples are reported in table 1a.

Some results will be compared to previous results from very low frequency ultrasonic measurements by Fraser [50] on two samples which are also presented in table 1b.

3. Results

3.1. Room temperature measurements: influence of fictive temperature

First, samples from set A having different fictive temperatures were measured at room temperature in order to determine their longitudinal sound velocity. Figure 1 shows that the longitudinal Brillouin peak increases when the fictive temperature increases from 1373 to 1773 K.

Figure 2 shows longitudinal sound velocity versus fictive temperature for samples A annealed from 1173 to 1773 K. The evolution of the refractive index n with fictive temperature (table 1a) has been taken into account for the calculation of V_L. It appears that for silica glass V_L increases linearly by 8.8×10^{-2} m s^{-1} K^{-1} with increasing fictive temperature in the range 1173–1773 K—apart from the sample having a fictive temperature of 1773 K, probably associated with an artefact or constraints. Using this linear relationship, the fictive temperature of the as-received sample A is thus found to be equal to 1653 ± 10 K. This result is consistent with the previous Raman and IR estimation equal to 1643 ± 40 K [46, 47].

Results of low frequency ultrasonic measurements from Fraser [50] on silica samples containing few OH groups (IR Vitreosil)—similar to sample A—are also shown in figure 2. It must be noted that difference in frequency between Fraser and our measurements can partly account for the difference in sound velocity [53, 54]. For IR Vitreosil V_L and for sample A, fictive temperature dependences are parallel.

Figure 3 shows longitudinal sound velocity plotted this time as a function of density for different heat treated samples: samples A from this study and IR Vitreosil from Fraser [50]. It appears that almost independently of the nature of the samples, V_L evolves with density with a variation close to 7.2×10^{-3} m^4 s^{-1} g^{-1}. Then, V_L increases almost linearly with both fictive temperature and density which is consistent with the idea of a linear increase of density with T_F (below 1673 K).

3.2. In situ temperature measurements: influence of temperature

Figure 4 shows variations in longitudinal sound velocity with temperature across the glass transition interval. Two different analyses of Brillouin shift data as a function of temperature

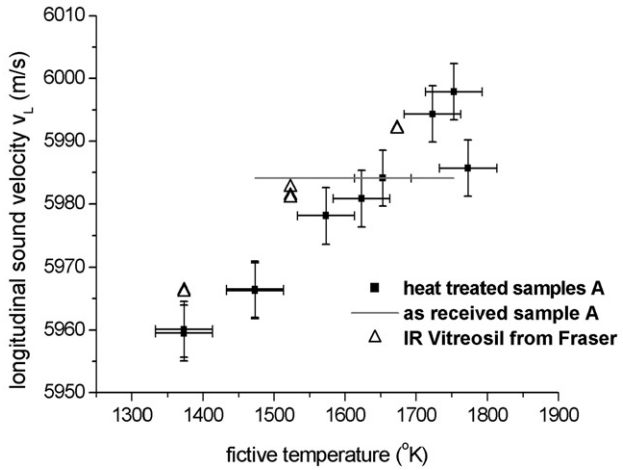

Figure 2. Room temperature longitudinal sound velocity for sample A (■) versus fictive temperature measured by high resolution Brillouin spectroscopy. The full line gives the position of the as-received sample A. The ultrasonic results from Fraser [50] on a silica glass containing a low OH concentration (table 2) are also presented for comparison on this figure and will be referred to in section 5.

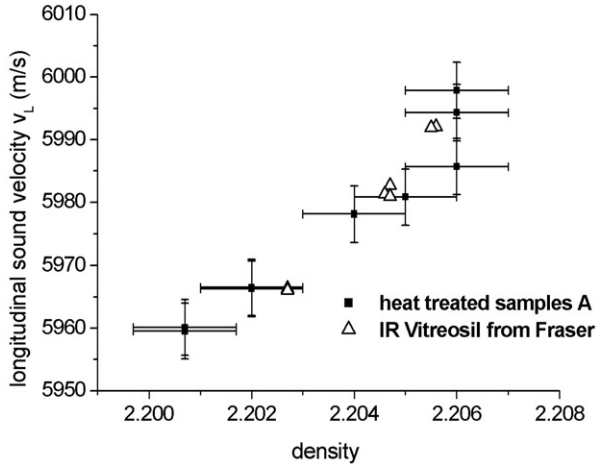

Figure 3. Room temperature longitudinal sound velocity versus sample density for sample A (■) and for IR Vitreosil measured by Fraser [50] (table 1a). Differences in density occur from variations in fictive temperature rather than from variations in OH concentration (IR Vitreosil has 2.4 ppm OH and sample A contains a few ppb OH).

are compared. In most data of the literature n is taken independent of T. However, it is important to consider the evolution of n with temperature [19] because differences between the two analyses are significant, in particular at high temperature (at 1773 K the difference between the two analyses is of the order of 175 m s^{-1} whereas the variation in sound velocity in the range 300–1773 K is around 540 m s^{-1}).

Figure 5 shows comparison of the temperature dependence of the longitudinal sound velocity in the range 300–1773 K for two samples A, having fictive temperatures equal,

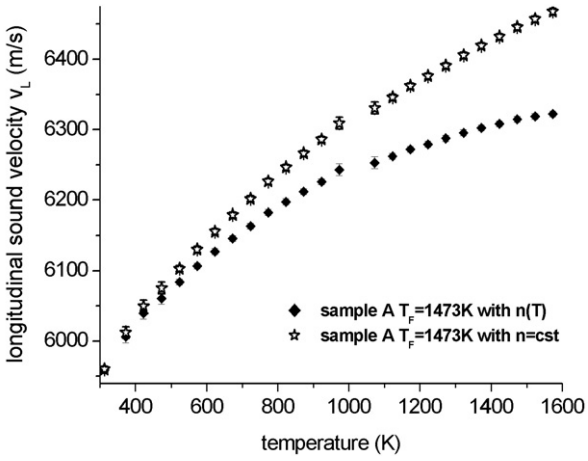

Figure 4. Sound velocity versus temperature for sample A: comparison between an analysis with $n(T)$ and an analysis with $n =$ constant.

respectively, to 1773 and 1473 K. Measurements have been performed while heating at a rate of about 1.30 ± 0.05 K min^{-1} whereas spectra are measured during isothermal annealing within 10 min. We considered for this calculation that $n(T)$ increases with temperature, following the interpolation of thermal dependence from [19]. A continuous increase is observed for V_L but the slope becomes smaller at high temperature. The sample having a higher fictive temperature has a higher sound velocity up to approximately 973 K, then the two curves join together and a small difference in sound velocity is again observed from 1273 to 1573 K. The difference between the two curves has been plotted on figure 6 to emphasize the influence of T and T_F. The bump in the range 1273–1773 K may be attributed to structural relaxation in the glass transformation range. However, the difference at room temperature which decreases with increasing temperature and vanishes at 973 K is a new feature.

In order to show that the structural relaxation effect gives rise to variations in longitudinal sound velocity, we have measured *in situ* isothermal evolution of the longitudinal Brillouin shift at an annealing temperature 1448 K (figure 7) as a function of time, after fast cooling of the sample from 1773 K. The stabilization time, found to be equal to 400 min at 1448 K, lies in the interval 105–4320 min corresponding, respectively, to the heat treatment times used for the stabilization of samples A1200 and A1100. Although the changes are small (about 6 m s^{-1}), almost of the order of the experimental error, the data can be well fitted by a decreasing exponential law, in agreement with a relaxation process with a characteristic time equal to 156 min.

The same *in situ* relaxation measurement was also performed at 1448 K by SAXS [42, 55]. The relaxation of the density fluctuations has also been fitted using an exponential decay and gives a characteristic decay time equal to 36 min. So the characteristic decay time for sound velocity seems much longer than the decay time for density fluctuations during isothermal relaxation at the same temperature. This difference can be explained, apart from a possible difference in the measurements of the furnace temperature (the highest error in temperature is found to be equal to 5 K), by the different length scales associated with the two experiments (Brillouin scattering is a macroscopic probe whereas the SAXS probe length scales corresponding to the medium range order).

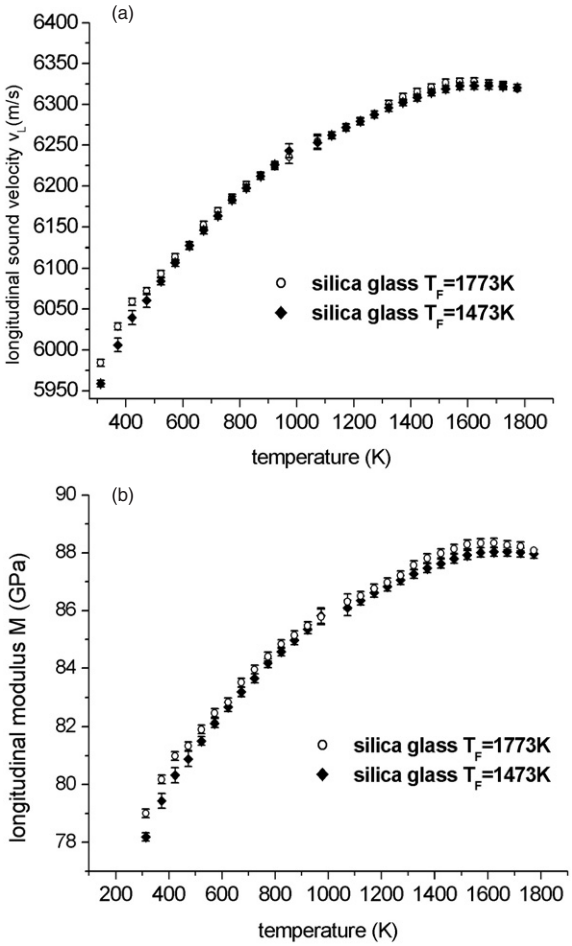

Figure 5. Longitudinal sound velocity (a) and longitudinal modulus (b) measured for two samples A heat treated at temperatures T_a respectively equal to 1473 K (diamond) and 1773 K (open circle). Error bars are calculated taking into account the error in shift determination and in scattering angle variation. Some larger error bars are related to a poorer Brillouin shift extraction due to a difficult deconvolution between the elastic line and the Brillouin line.

3.3. Influence of the OH content

The second part of the results concerns the influence of hydration on longitudinal and transverse sound velocity in silica glasses. Figure 8 shows room temperature longitudinal sound velocity V_L versus OH content for different samples (B, C, D, E, F). Longitudinal sound velocity, V_L, tends to decrease with increasing OH content (figure 8), yet some differences for very low OH content may be due either to other impurities or to fictive temperature. For a high OH content the amount of other impurities seems to have a negligible effect.

OH content is often related to relaxation processes when water diffusion is thermally activated [56]. The temperature dependence of the longitudinal and transversal sound velocity has been measured for the more hydrated (sol–gel glass) and two dehydrated silica glasses. Results for longitudinal sound velocity are shown in figure 9. Within the accuracy of the experiments, the temperature dependences of longitudinal sound velocity are similar for the

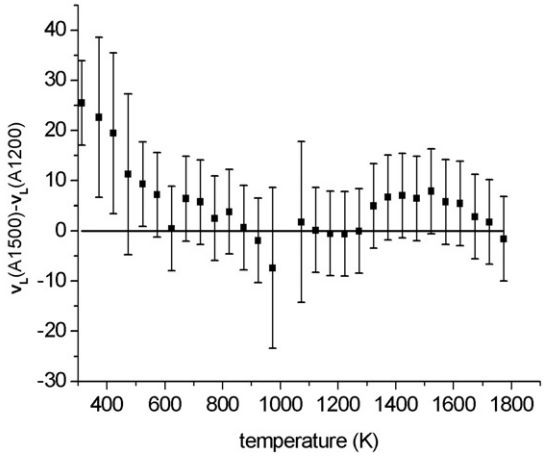

Figure 6. Longitudinal sound velocity difference between sample A, $T_F = 1773$ K, and sample A, $T_F = 1473$ K. The horizontal line is a guide for the eye giving a difference equal to zero.

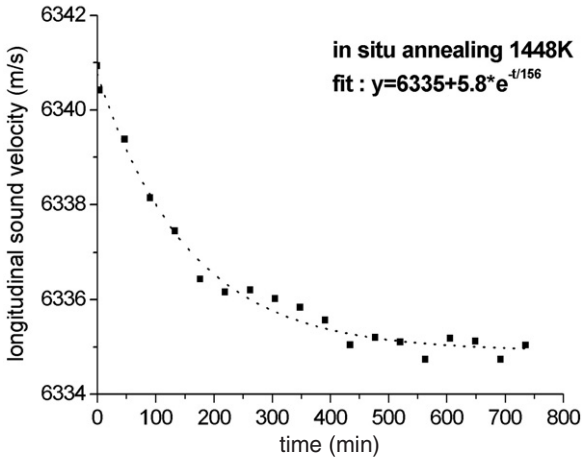

Figure 7. Longitudinal sound velocity measured isothermally at 1448 K versus time for a sample fast cooled from 1773 K to erase its thermal history.

three samples apart from a slight kink which is observed in the sol–gel glass around 1173 K. In the same figure, data from room temperature to 1773 K are also compared to data from Polian [10] reanalysed with the same temperature dependence of refractive index taken from Bruckner [19] as used for the other samples. The thermal dependence found is slightly higher than the one observed for our samples. The comparison with the data from Polian [10] extends the temperature range of our measurements toward very high temperatures and lets a small decrease of the sound velocity appear above 1800 K, and shows the existence of a maximum value for V_L between 1500 and 1800 K.

The transverse sound velocity for samples B and D is compared in figure 10. For the sol–gel silica, transverse sound velocity is about 35 m s^{-1}, whereas longitudinal sound velocity is 90 m s^{-1}, lower than for the commercial sample B. A maximum is observed for the two samples, at 1373 K for sample B and at 1173 K for sample D. For temperatures above this

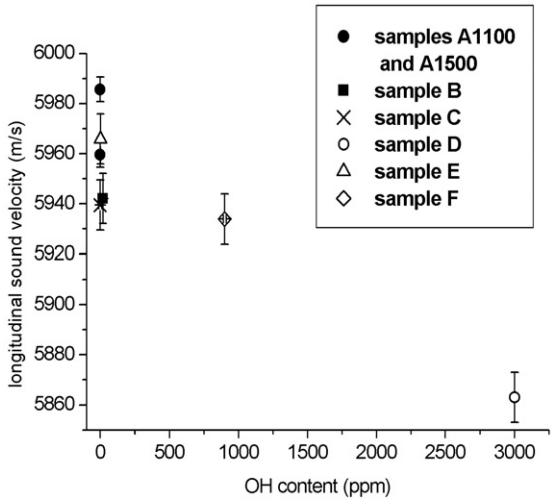

Figure 8. Room temperature longitudinal sound velocity versus OH concentration for some silica glasses presented in table 2. For samples A (full squares) two fictive temperatures have been shown in order to give a scale of variations due to OH as compared to variation due to fictive temperatures. Errors bars are taking into account a large uncertainty in n for samples B, C, D, E, F.

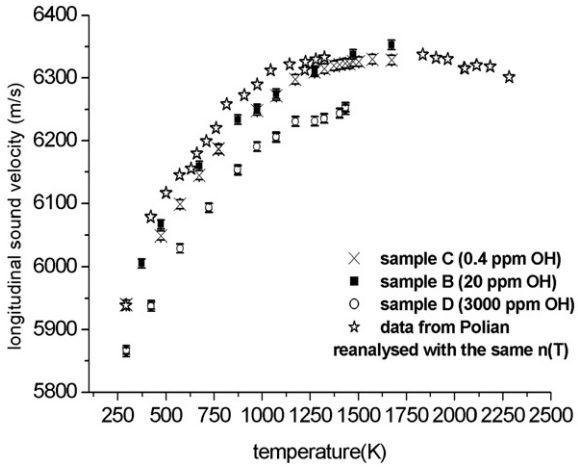

Figure 9. Longitudinal sound velocity calculated from high resolution Brillouin scattering up to 1773 K for three samples characterized by different OH concentrations (table 1a). We also show a comparison with data from Polian [10] up to 2273 K, reanalyzed with $n(T)$ extracted from Bruckner [19].

maximum, the transverse sound velocity starts to decrease for the two glasses, very clearly for the sol–gel glass. The comparison with the data from Polian [10] reanalysed with $n(T)$ used for the samples studied confirms this decrease, provided $n(T)$ can be extrapolated from [19] at temperatures as high as 2000 K.

Longitudinal M and shear G moduli can be deduced, respectively, from longitudinal and transverse sound velocity using equations (3) and (4). The compression modulus K can then be calculated using equation (5). Figure 11 shows all three moduli calculated for samples B (Puropsil A) and D (sol–gel). As for longitudinal and transverse sound velocity, the temperature

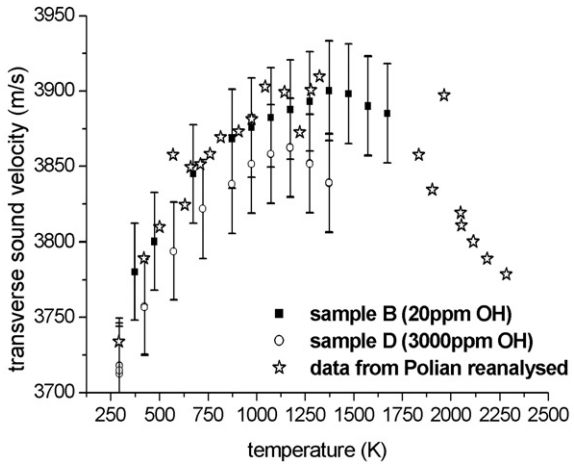

Figure 10. Transverse sound velocity deduced from high resolution Brillouin scattering data up to 1773 K for three samples characterized by different OH concentrations (table 1a). We also show a comparison with data from Polian [10] up to 2273 K, reanalyzed with $n(T)$ extracted from Bruckner [19].

dependences of the bulk modulus for sample D and for sample B are parallel; the amplitude of the modulus for sample D is shifted by 3–5% downward. The bulk modulus is always increasing with T even in the glass transition interval, whereas the shear modulus decreases for temperatures higher than 1173 K.

Adiabatic compressibility at infinite frequency β_∞ can be calculated from the inverse compression modulus (equation (5)) for Puropsil A (sample B) and for sol–gel silica (sample D), considering that the density of silica is almost constant with temperature. The variations of the modulus induced by the increase in density with temperature are within the error bars and can be neglected. Figure 11(d) shows results for the adiabatic compressibility for samples B and D versus increasing temperature. The comparison of the thermal dependence of compressibility for the two commercial glasses with data from Polian [10] are in general agreement within experimental uncertainty, provided they are reanalyzed using the same temperature dependence of the refractive index [19].

4. Interpretation

4.1. Sound velocity and moduli amplitude at room temperature: influence of fictive temperature and OH content

In silica glass, we find that longitudinal sound velocity increases with increasing fictive temperature as a result of increase in both the Brillouin shift ($\Delta\nu = 0.155$ GHz–$\Delta\nu/\nu = 0.45\%$ for $\Delta T_F = 400$ K) and the refractive index ($\Delta n/n = 0.03\%$ for $\Delta T_F = 400$ K). This evolution of V_L with T_F for silica glass can be considered as anomalous if compared to alkali silicates, borate and phosphates glasses for which sound velocities decrease with increasing temperature. Few measurements, mostly Brillouin scattering measurements, have been reported in the literature about the effect of thermal history on acoustic properties [34, 57–61]. For the different glasses reported in literature, sound velocity strongly decreases with increasing stabilization temperature.

Table 2 presents quantitative comparison of $(\Delta V_L/V_L)/(\Delta T_F/T_F)$ for different glasses compared to the relative ratio $(\Delta\rho/\rho)/(\Delta T_F/T_F)$ and $(\Delta n/n)/(\Delta T_F/T_F)$. It appears at first

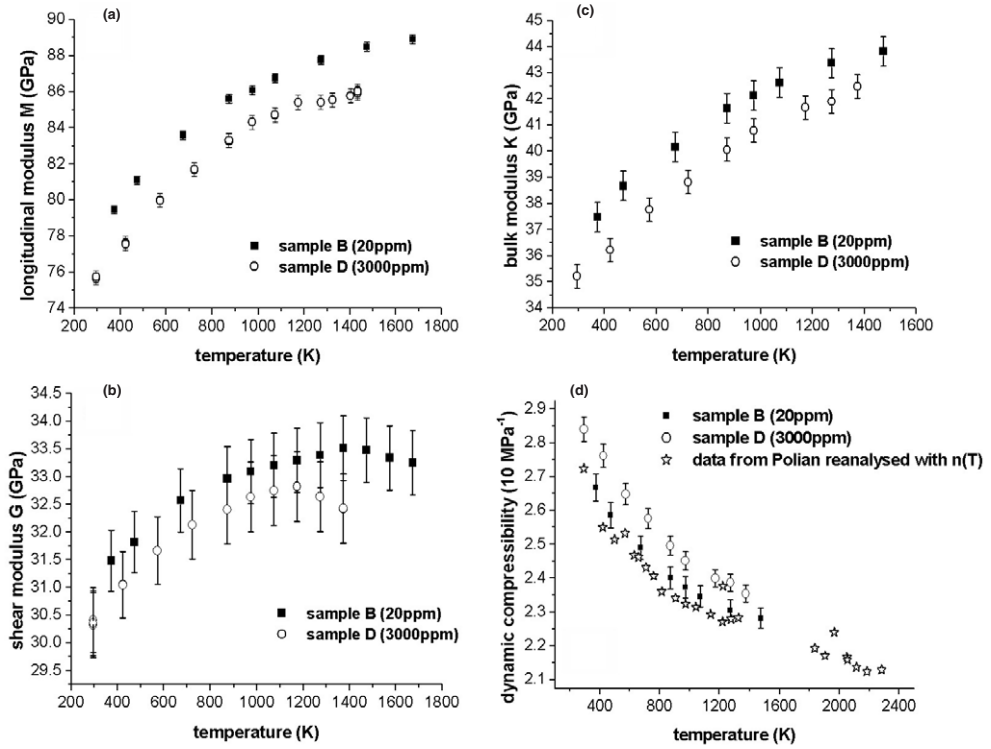

Figure 11. Longitudinal (a), transverse (b), bulk (c) moduli and adiabatic compressibility (d) for sample B (full squares) and D (open circles) versus temperature.

Table 2. Quantitative influence of fictive temperature on density ρ, refractive index n, longitudinal sound velocity V_L and amplitude of density fluctuations $I(0)$ for different glasses.

	ΔT_F (K)	$(\Delta\rho/\rho)/(\Delta T_F/T_F)$	$(\Delta n/n)/(\Delta T_F/T_F)$	$(\Delta V_L/V_L)/(\Delta T_F/T_F)$	$(\Delta I(0)/I(0))/(\Delta T_F/T_F)$
B_2O_3 glass, dry [57]	530–560= 30	-3.0×10^{-1}	—	-1.6	
Float glass [55]	753–893= 140	-5.4×10^{-2}	—	-1.0×10^{-1}	5.4×10^{-1}
Sovirel glass [34]	858–1023= 165	—	-2.1×10^{-2}	-2.3×10^{-1}	
Silica sample A	1373–1773= 400	$+8.9 \times 10^{-3}$	$+1.1 \times 10^{-3}$	$+2.6 \times 10^{-2}$	3.8×10^{-1}

that variations in silica glass have an opposite sign compared to variations in the three other glasses. Secondly, those three ratios are lower for glasses having increasing ΔT_F. Then silica glass shows the smallest relative variation of longitudinal sound velocity but also the smallest relative density and refractive index variation versus fictive temperature. The variation of V_L with T_F in silica glass is one order magnitude lower than in the other glasses and can be related to the very small slope for the thermal dependence of V_L in the range 1373–1773 K, whereas for B_2O_3 and the other glasses the variation of V_L in the glassy transition range is quite important [57].

We have shown that for silica glasses having different fictive temperatures, a linear relationship can be found between density and sound velocity. Such an evolution is not particular to silica glass: Ramos show that both V_L and V_T in borate glasses having different thermal histories increase almost linearly with increasing density [57]. As a matter of fact,

an increase in longitudinal sound velocity for different silica samples progressively densified under high pressure or permanently densified has also been observed [2, 62]. Thus, for silica glass both sound velocity and density increase with increasing T_F, whereas for other silicate and borate glasses both sound velocity and density decrease with increasing T_F. It seems that anomalous behaviour of silica sound velocity is mostly related to the anomalous densification versus T_F.

The anomalous density behaviour in silica glass with increasing T_F can be explained by the modification of the local and intermediate range structure. Local structural modification has been studied through vibrational IR and Raman spectroscopy. The shifts of the peak related to stretching vibration of the Si–O [31, 28–30, 46, 63] bonds, within Si–O–Si angles, are interpreted by a slight decrease of the inter-tetrahedral Si–O–Si angles θ distributed around a mean value. This decrease has been estimated ($\Delta\theta$ of the order of 2° for ΔT_F of the order of 400 K) from Raman scattering [63] and from IR spectroscopy [27]. At intermediate range, the silica glass structure can be described by the occurrence of rings containing from three to nine tetrahedra. The two sharp peaks, so-called 'defect lines', D_1 and D_2 observed in the Raman spectrum at 495 and 606 cm^{-1} have been associated with the vibrations of three and four membered rings. The intensification of the two lines with increasing fictive temperature—or with densifying under pressure or irradiation [63]—has been interpreted by a modification of those ring populations [64], but this interpretation has been counterbalanced [65]. Molecular dynamics simulations for glasses obtained with different quenching rates also show a modification of ring statistics with quenching rate, although fictive temperatures of simulated glass are very high compared to experimental ones [65, 42]. This modification of ring statistics in favour of smaller ones would be consistent with a decrease in the mean Si–O–Si angle and thus a densification with increasing T_F.

Small composition effects such as OH content also influence the properties of silica glass such as acoustic properties (longitudinal and transverse sound velocities). Our results (figure 9) are consistent with ultrasound measurements: Kushibiki has shown that a sample containing 860 ppm OH (and 30 ppm Cl) has longitudinal and transverse sound velocities respectively 57 and 5 $m\,s^{-1}$ lower than for an OH-free sample [66]. Both density and V_L decrease with increasing OH content in silica glass through an apparently linear relationship. The decrease in density with the incorporation of OH groups can be explained by the disruption of the continuous covalently bonded SiO_4 network.

Finally, if the fictive temperature effect and the OH content effect are compared at room temperature, within the fictive temperature range and the OH content range available, the influence of fictive temperature ($\Delta V_L = 40\ m\,s^{-1}$ in the range of experimentally available temperature $\Delta T_F = 400\,°C$) is less important than the influence of a large number of hydroxyls ($\Delta V_L = 90\ m\,s^{-1}$ for $\Delta[OH] = 3000$ ppm). When OH content is low, the influence of other impurities such as Cl is apparently no longer negligible, as shown by the amplitude of the sound velocity for sample C (Suprasil) being out of the general tendency. This sample is characterized by a lower elasticity than samples having the same OH content but which are Cl free. Impurities tend to modify the structure, in the case of OH and Cl a softening is observed.

4.2. Thermal dependence of sound velocity and modulus amplitude

As for the T_F dependence, the temperature dependence of sound velocity in silica glass increases with increasing temperature. This positive slope, also reported for some other tetrahedral glasses such as GeO_2 (observed for all silica glass samples and all type of moduli below the glass transition range) is anomalous compared to other usual glasses (borosilicate or float glasses).

SiO_2 and GeO_2 are both glass formers with highly connected networks. According to Kul'bitskaya [20], the difference between those glass formers and their alkali derived glasses can be explained by the increase in the number of non-bridging oxygens in multicomponent glasses; modifying oxides disturb the continuity of the network in favour of inhomogeneous regions. For example, in $(NaO_2)_x(SiO_2)_{1-x}$ the anomalous positive thermal dependence disappears for sodium oxide content x higher than 0.16 [60].

B_2O_3 is also a simple glass former but does exhibit normal elastic properties [20, 57]. In fact, its structure consists of a highly connected planar triangle network instead of a highly tetrahedrally networked structure. Then it appears that the anomalous thermal dependence of the elastic moduli in silica and germania glasses are strongly correlated to the highly connected tetrahedral network and to the nature of the link between atoms [20, 67].

The comparison of the thermal dependence of acoustic properties for two different fictive temperatures gives another insight into the peculiar behaviour of silica glass. Acoustic properties in usual glasses such as float or barium glass have the following behaviour:

- Low fictive temperature glass and high fictive temperature glass have different sound velocities at room temperature [34, 55].
- When temperature increases for $T < [T_g]$, *thermal dependence of* V_L appears to be translated toward lower values when fictive temperature increases but with the same thermal dependence.
- For $T > [T_g]$ the thermal history effect vanishes, structures and properties are in equilibrium and V_L is the same for samples having different T_F.
- In the glass transition interval, singular effects, such as hysteresis or kinks [3–5, 34, 55] around T_g, are expected for samples having different thermal histories, even if those different thermal histories do not lead to measurable differences at room temperature. These singularities may appear when the rate of configurational change becomes of the order of magnitude of the heating rate, and traduces the attempt of the glass to adjust its molecular configuration as the temperature is changed.

In silica glass, the influence of fictive temperature on the moduli does not, in contrast to other glasses, give rise to a simple curve translation in the glassy range. The influence of fictive temperature can be observed through small amplitude differences below 873 K and also in the glass transition region. Samples A1200 and A1500 are different at room temperature, but the curves join as early as 873 K and finally a small difference can be detected around T_g from 1373 to 1673 K.

New remarks also come from the comparison of the thermal dependence of acoustic properties for glasses containing very low and very high concentration of hydroxyls. For sol–gel silica glass, the amount of hydroxyl is very high and the sample differentiates with a smaller value of sound velocity, and in the glass transition range, V_L shows a plateau and V_T a maximum.

Actually for transverse sound velocity the maximum is observed in both sol–gel glass and Puropsil, respectively, around 1173 K and 1373 K. The existence of a maximum in the range 1373–1773 K is confirmed while plotting data from Polian [10] up to 2300 K reanalysed with the temperature dependence of the refractive index. This maximum occurs in the glass transition range. It is consistent with a negative fictive temperature dependence measured by Fraser [13] for V_T. This decrease observed in the glass transition range for V_T and G may be connected to a structural relaxation assisted by the hydroxyls. A structural softening may also contribute to the decrease of V_L. As a matter of fact, V_L is linked at the same time to K (compressibility) and to G (shear) (equation (5)). Then the plateau observed for V_L results from a compressibility which keeps on increasing with temperature whereas the shear modulus G is decreasing.

Table 3. Comparison of SAXS intensity $I(q = 0)$ and sound velocity for silica glass and float glass for samples heat treated at temperatures corresponding to equivalent viscosities.

	A1200	A1500	Sample E	Sample F	Float glass [55]	Float glass [55]
T_F or [OH]	1200 °C	1500 °C	2 ppm	900 ppm	480 °C	620 °C
$I(0)$ e.u./molecule	20.6	23.3	20	18.2	11.3	13
V_L (300 K) m s^{-1}	5985	5998	5972	5940	6930	5925

5. Discussion

5.1. Comparison between density fluctuations and Kul'bitskaya's model [20]

Fluctuations originating from the change of the dielectric constant (dielectric susceptibility and polarizability, electronic densities) associated with local density fluctuations can account for the scattering of electromagnetic waves in glasses. Then it seems right to consider a model which tries to give a semi-quantitative explanation of the positive temperature dependence of the elastic modulus in silica glass trough the existence of spatial fluctuations like the model established by Kul'bitskaya [20]. This model assumes that glass is composed of inhomogeneities resulting from the freezing-in of natural fluctuations around the glass transition. It is demonstrated that, in an elastic inhomogeneous medium, an effective elastic modulus ε_{eff} can then be written as the difference of two terms: an average modulus ε_0 and a correction term depending on the amplitude of those fluctuations $\langle\Delta^2\rangle$ (equation (8)).

$$\varepsilon_{\text{eff}} = \varepsilon_0 - \langle\Delta^2\rangle. \tag{8}$$

The temperature dependence of the sound velocity in silica glass and in float glass (for comparison) can be discussed in the frame of equation (8) considering a possible correlation between the density fluctuations $(\Delta\rho)^2/\rho$ measured by SAXS in the same samples [42, 51, 69] and the fluctuation term $\langle\Delta^2\rangle$ evoked in equation (8).

It has been demonstrated experimentally by SAXS [42, 51, 52, 69] that density fluctuations increase in silica glass much more with fictive temperature (38%) than the average density (0.89%) for the same fictive temperature range (tables 2, 3). Then, if the fluctuation term $\langle\Delta^2\rangle$ is considered to evolve in the same way as the density fluctuation term, $(\Delta\rho)^2/\rho$, this term is expected to increase with the freezing-in temperature for both glasses. The decrease imposed by the term $-\langle\Delta^2\rangle$ should induce a decrease of the effective moduli ε_{eff}, if the average modulus ε_0 is supposed to evolve like the average density of the glass. This result is inconsistent with the experimental observation showing that the sound velocity V increases with fictive temperature in silica glass.

For float glass, it has been demonstrated [55, 68] that density fluctuations increase faster (54% if the dependence of the concentration fluctuations on T_F is neglected) than the average density (5.4%) decreases with fictive temperature (tables 2, 3). Then it can be assumed that the dependence of effective modulus on fictive temperature is determined by the term $-\langle\Delta^2\rangle$. Thus the decrease of the effective modulus is consistent with the experimental observation.

The thermal dependence of the effective modulus can also be discussed assuming the same correlation. The density fluctuation term increases with temperature. If variation of the average modulus ε_0 may be related to the thermal expansion coefficient, being very small for silica as postulated by Kul'bitskaya, we can conclude that $\mathrm{d}\varepsilon_{\text{eff}}/\mathrm{d}t \sim -\mathrm{d}\langle\Delta^2\rangle/\mathrm{d}T$. Thus the effective modulus would decrease with temperature in silica glass whereas the purpose of Kul'bitskaya's model was to demonstrate the positive temperature dependence of the effective modulus (i.e. sound velocity) observed experimentally. For float glass the experimental negative thermal dependence is well described by the model.

The evolution of the elastic modulus versus OH content can also be discussed in the same framework. SAXS measurements have shown that an increase in the OH content by 900 ppm induces a decrease of $(\Delta\rho)^2/\rho$ by about 10% [52], whereas the average density ρ is expected to increase by 0.02%. It seems difficult then to explain the decrease in longitudinal sound velocity with increasing OH for glasses containing a high amount of OH, such as sol–gel silica.

To summarize, for silica glass, when the elastic fluctuation term and the density fluctuation are supposed to be correlated, the effective moduli do not evolve with temperature/fictive temperature in the way predicted by Kul'bitskaya.

Thus if the fluctuation term $\langle\Delta^2\rangle$ in the Kul'bitskaya model is responsible for the anomalous positive thermal dependence of the elastic moduli in silica glass, something other than density fluctuations must be responsible for the origin of this term. In the thermal dependence of V_L shown in the results for silica glass, the two glasses having different thermal histories join at quite a low temperature. This effect seems to demonstrate that a relaxation of $\langle\Delta^2\rangle$ or of ε_0 may occur at temperatures much lower than the temperatures of the glass transition interval. These very low temperatures are associated with high viscosities and also huge relaxation times, so these low temperature relaxations can hardly be associated with relaxations from structural entities such as frozen-in density fluctuations. In the following paragraph different a hypothesis is developed.

The fluctuation term in Kul'bitskaya's model could be correlated to elastic fluctuations which do not involve any density fluctuation. Such elastic fluctuations might be bound with residual stress or with fluctuations of the elastic strength of the Si–O bond without any change in the bond length. In the case of residual elastic stress, an increasing temperature should decrease the stress and thus the decreasing term $-\langle\Delta^2\rangle$ is expected to induce an increase in the effective modulus. The low temperature relaxation, mentioned in the presentation of figure 5, could be linked to such an elastic relaxation process.

Recent results from numerical simulations are consistent with the hypothesis of a heterogeneous nature of glass from a dynamical point of view [70, 71]. These dynamic simulations in Lennard-Jones systems have shown that dynamic heterogeneities do exist, not only in the supercooled liquid as already established [72–74] but also in the glassy state for all temperatures. Mobile and immobile particles have been studied: both kinds of particles form clusters. Results from Rossi [75] show the existence of an inhomogeneous cohesion (heterogeneities in the elastic constant) on the nanometre scale in glass. The existence of some nanoscaled regions of low and high cohesion was proposed formerly by Duval [76, 77] in order to explain the origin of the boson peak.

The model from Kul'bitskaya explains the elastic properties of usual glasses through a mean field approach. Usual glasses (like float glass) are often very complex glasses containing many components for which a mean field approach is suitable. As a matter of fact, we can suspect that even the most different configurations are not so far from the average configuration as they are in a glass like silica (for example in silica glass the angular distribution ranges from 120° to 180°). Thus simple glasses like silica or germania, have very rigid networks for which this mean field approach may be less suitable, and topological or structural models are then necessary.

5.2. Glass polyamorphism

Several references are found in literature pointing out a strong correlation between elastic properties of silica glass and those of its crystalline counterparts. A change between 773 and 873 K in the temperature dependence of the elastic moduli in silica glass has been reported in the derivation of the Landau–Placzek ratio [6] and in the adiabatic compressibility

around 900 K [10]. This change has been interpreted as a reminder of the α–β quartz transition [6] (linked with the presence of some quartz crystallites associated with the fused quartz elaboration process of the samples). The change in the elastic moduli has not been observed in any of the silica glasses studied, but the change of slope in the adiabatic compressibility can be observed in samples B and D.

The concept of polyamorphism in silica glass has been introduced to illustrate the fact that silica glass could be described like a mixture of a finite number of energetically distinct structural states [78]. Early models are based on the assumption of the existence of two energetically distinct structural states, in order to explain the very low temperature specific properties of silica glass through the tunnelling systems between two energy wells (corresponding to the two structural states often associated with states of crystalline silica polymorphs) [1].

Cristobalite has always been a favoured archetype for a structural model of silica glass (Si–O–Si angles, average ring size, etc) for many simulations. Huang and Kieffer [78] have studied amorphous transitions under various thermomechanical conditions with molecular dynamic simulations and reproduce various anomalies of elastic properties in pressure or temperature dependence. Their simulations reveal that thermomechanical anomalies of silica glass are due to a localized reversible structural 'transition' close to those observed in the α–β cristobalite phase transformation. This 'transition' would involve Si–O–Si bond rotation and thus would take place without any change in the local order (bond length and angles, ring size distribution) but would affect ring geometry that becomes more symmetric under expansion. As the α-cristobalite phase is characterized by a lower modulus than the β-phase, when a proportion of the angles undergo a rotation into the β configuration (determined by increase in pressure and temperature) the elastic modulus increases. The idea of tetrahedron rotations has already been proposed by Buchenau [79] in order to explain low frequency vibrational modes. Anomalous density behaviour has also been related to a transition from a low density amorphous state to a high density amorphous state [48, 49].

The increase of the modulus with increasing fictive temperature could thus be explained by a larger number of local entities which have been undergoing transformation into the β configuration. The β-cristobalite phase is a high temperature disordered phase and it seems consistent to associate this phase with a glass having a high fictive temperature. However, the β-cristobalite phase has a lower density than the α-cristobalite phase, and it is thus expected that a higher number of β-cristobalite configurations decrease the density, which is in disagreement with the increase of density observed in silica glass when T_F increases.

As for the sound velocity when OH content increases, it has been demonstrated that OH favours local relaxation in glass [56]; thus if a stressed region contains some OH bonds the relaxation process may happen through OH relaxation rather than through the rotation process, thus locally the modulus may not increase as the rotation process is not involved.

6. Conclusion

High resolution Brillouin scattering was used to monitor the variation induced by fictive temperature and OH content in the elastic properties of silica glass at room temperature and versus increasing temperature up to and across the glass transition. The thermal dependence of the elastic moduli is found to be positive in the glassy range whatever the T_F and the OH content. Yet in the glass transition range, the most hydrated samples show a slight decrease in the transverse elastic moduli beyond 1223 K. Those hydrated samples also show lower moduli. The positive temperature dependence of the elastic moduli in silica glass, in contrast to usual glasses which show negative thermal dependence, is one of the numerous anomalies reported

for silica glass. Furthermore, we demonstrate in this study the increase in the sound velocity with increasing fictive temperatures in silica glass, which also emphasizes the anomalous character of silica glass. The results have been discussed through the phenomenological model of the fluctuations proposed by Kul'bitskaya [20] and the structural model inspired by the α–β cristobalite transition proposed by Huang [78]. The description of the results does not apply well to silica glass by simply considering that the fluctuation term equals the amplitude of the density fluctuation; an independent elastic term should probably be considered. The description of the structure by a localized reversible structural 'transition/rotation' seems to give interesting clues to understanding the influence of fictive temperature and OH content. Future improvement in the understanding of the link between the structural modifications and glass elastic properties is expected thanks to the involvement of simulation in the description of glass behaviour.

Acknowledgments

The work has been carried out with the help of S Clement in the preparation of the heating device and optical measurements. We acknowledge L Vaccarini for involvement in measurements. We also wish to thank B Ruffle and R Vialla for helping in the setup of the Brillouin device, and R Vacher for the apparatus design. Finally, we thank R Brüning for lending some silica glass samples.

References

[1] Vuckcevich M R 1972 *J. Non-Cryst. Solids* **11** 25
[2] Polian A and Grimsditch M 1993 *Phys. Rev.* B **47** 13979
[3] Askarpour V, Manghnani M H and Richet P 1993 *J. Geophys. Res.* **98** 17683
[4] Vo-Thanh D, Polian A and Richet P 1996 *Geophys. Res. Lett.* **23** 423
[5] Xu J-A, Manghnani M H and Richet P 1992 *Phys. Rev.* B **46** 9213
[6] Bucaro J A and Dardy H D 1974 *J. Appl. Phys.* **45** 5324
[7] Pelous J and Vacher R 1975 *Phys. Lett.* A **53** 233
[8] Krol D M, Lyons K B, Abrawer S and Kurkjian C 1986 *Phys. Rev.* B **33** 4196
[9] Youngman R E, Kieffer J, Bass J L and Duffrene L 1997 *J. Non-Cryst. Solids* **222** 190
[10] Polian A, Vo-Thanh D and Richet P 2002 *Europhys. Lett.* **57** 375
[11] Fukuhara M and Sanpei A 1994 *Japan. J. Appl. Phys.* **33** 2890
[12] Krause J T and Kurkjian C R 1968 *J. Am. Ceram. Soc.* **51** 226
[13] Fraser D B 1970 *J. Appl. Phys.* **41** 6
[14] Marx W and Silvertsen J M 1953 *J. Appl. Phys.* **24** 81
[15] Vacher R, Pelous J, Plicque F and Zarembovitch A 1981 *J. Non-Cryst. Solids* **45** 397
[16] Tielburger D, Merz R, Ehrenfels R and Hunklinger S 1992 *Phys. Rev.* B **45** 2750
[17] Levelut C, Le Parc R and Pelous J 2006 *Phys. Rev.* **73** 052201
[18] Anderson O L and Dienes G J 1958 *Non Crystalline Solids* ed V D Fréchette (New York: Wiley) p 449
[19] Bruckner R 1970 *J. Non-Cryst. Solids* **5** 123
[20] Kul'bitskaya M N, Nemilov S V and Shutilov V A 1975 *Sov. Phys.—Solid State* **16** 2319
[21] Babcock C L, Barber S W and Fajans K 1954 *Ind. Eng. Chem.* **46** 161
[22] Tool 1953 *J. Am. Ceram. Soc.* **29** 240
[23] Kakiuchida H, Saito K and Ikushima A J 2004 *Japan. J. Appl. Phys.* 2 **43** L743
[24] Kakiuchida H, Saito K and Ikushima A J 2003 *J. Appl. Phys.* **94** 1705
[25] Kakiuchida H, Saito K and Ikushima A J 2003 *J. Appl. Phys.* **93** 777
[26] Ryu S R and Tomozawa M 2006 *J. Am. Ceram. Soc.* **89** 81
[27] Koike A, Ryu S R and Tomozawa M 2005 *J. Non-Cryst. Solids* **351** 3797
[28] Tomozawa M, Hong J W and Ryu S R 2005 *J. Non-Cryst. Solids* **351** 1054
[29] Kim D L and Tomozawa M 2001 *J. Non-Cryst. Solids* **286** 132
[30] Agarwal A and Tomozawa M 1997 *J. Non-Cryst. Solids* **209** 166

[31] Shin D W and Tomozawa M 1996 *J. Non-Cryst. Solids* **203** 262
[32] Agarwal A, Davis K M and Tomozawa M 1995 *J. Non-Cryst. Solids* **185** 191
[33] Haken U, Humbach O, Ortner S and Fabian H 2000 *J. Non-Cryst. Solids* **65** 9
[34] Vacher R, Delsanti M, Pelous J and Cecchi L 1974 *J. Mater. Sci.* **9** 829
[35] private communication
[36] Saito K *et al* 2000 *J. Non-Cryst. Solids* **270** 60
[37] Saito K and Ikushima A J 1998 *Appl. Phys. Lett.* **73** 1209
[38] Saito K and Ikushima A J 2002 *J. Appl. Phys.* **91** 4886
[39] Hetherington G, Jack K H and Kennedy J C 1964 *Phys. Chem. Glasses* **5** 130
[40] Vacher R, Shickfus M V and Huncklinguer S 1980 *Rev. Sci. Instrum.* **51** 288
[41] Sussner H and Vacher R 1979 *Appl. Opt.* **18** 3815
[42] Le Parc R 2002 *PhD Thesis* Université de Lyon1, Villeurbanne
[43] Shelby J E 2004 *J. Non-Cryst. Solids* **349** 331
[44] Vollmayr K, Kob W and Binder K 1996 *Phys. Rev.* B **54** 15808
[45] Douglas R W and Isard J O 1951 *Soc. Glass Technol.* **35** 206
[46] Le Parc R, Champagnon B, Guenot Ph and Dubois S 2001 *J. Non-Cryst. Solids* **293–295** 366
[47] Champagnon B, Le Parc R and Guenot Ph 2002 *Phil. Mag.* B **82** 251
[48] Sen S, Andrus R L, Baker D E and Murtagh M T 2004 *Phys. Rev. Lett.* **93** 125902
[49] Champagnon B, Martinet C, Martinez V and Le Parc R 2006 *10th International Workshop on Disordered Systems (Molveno, Italy)*
[50] Fraser D B 1968 *J. Appl. Phys.* **38** 5868
[51] Le Parc R, Champagnon B, David L, Faivre A, Levelut C, Guenot Ph, Hazemann J L, Rochas C and Simon J P 2002 *Phil. Mag.* B **82** 341
[52] Brüning R, Levelut C, Faivre A, LeParc R, Simon J P, Bley F and Hazemann J L 2005 *Europhys. Lett.* **70** 211
[53] Zarzycki J 1982 *Les Verres et L'etat Vitreux* (Paris: Masson) p 168
[54] Herzfeld K F and Litovitz T A 1959 *Absorption and Dispersion of Ultrasonic Waves* (New York: Academic)
[55] Levelut C, Le Parc R, Faivre A and Champagnon B 2006 *J. Non-Cryst. Solids* at press
[56] Kakiuchida H, Saito K and Ikushima A J 2002 *Japan. J. Appl. Phys.* 1 **41** 2993
[57] Ramos M A, Moreno J A, Viera S, Prieto C and Fernandez J F 1997 *J. Non-Cryst. Solids* **221** 170
[58] Le Saout G, Vaills Y and Luspin Y 2002 *Solid State Commun.* **123** 49
[59] Clementin-de-Leusse C 2000 *PhD Thesis* Université de Monpellier II
[60] Vaills Y, Luspin Y and Hauret G 2001 *J. Non-Cryst. Solids* **286** 224
[61] Prat J L 1996 *PhD Thesis* Université de Monpellier II
[62] Rat E 1999 *PhD Thesis* Université de Monpellier II
[63] Bates J B, Hendricks R W and Shaffer L B 1974 *J. Chem. Phys.* **61** 4163
[64] Geissberger A E and Galeener K E 1983 *Phys. Rev.* B **28** 3266
[65] Rahmani A, Benoit M and Benoit C 2003 *Phys. Rev.* B **68** 184202
[66] Kushibiki J I, Wei T C, Ohashi Y and Tada A 2000 *J. Appl. Phys.* **87** 3113
[67] Kieffer J, Masnik J E, Reardon B J and Bass J D 1995 *J. Non-Cryst. Solids* **183** 51
[68] Levelut C, Faivre A, Le Parc R, Champagnon B, Hazemann J L and Simon J P 2005 *Phys. Rev.* B **72** 224201
[69] Levelut C, Faivre A, Le Parc R, Champagnon B, Hazemann J L, David L, Rochas C and Simon J P 2002 *J. Non-Cryst. Solids* **307–310** 426
[70] Vollmayr-Lee K and Zippelius A 2005 *Phys. Rev.* E **72** 041507
[71] Leonforte F, Boissiere R, Tanguy A, Wittmer J P and Barrat J L 2005 *Phys. Rev.* B **72** 224206
[72] Bohmer R 1998 *Curr. Opin. Solid State Mater. Sci.* **3** 378
[73] Ediguer M D 2000 *Annu. Rev. Phys. Chem.* **51** 99
[74] Sillescu H 1999 *J. Non-Cryst. Solids* **243** 81
[75] Rossi B, Viliani G, Duval E, Angelani L and Garber W 2005 *Europhys. Lett.* **71** 256
[76] Duval E, Boukenter A and Achibat T 1986 *Phys. Rev. Lett.* **56** 2052
[77] Mermet A, Surotsev N, Duval E, Jal J F, Dupuy-Philon J and Dianoux J 1996 *Europhys. Lett.* **36** 277
[78] Huang L and Kieffer J 2004 *Phys. Rev.* B **69** 224203
[79] Buchenau U, Prager M, Nucker N, Dianoux A J, Ahmad N and Phillips W A 1986 *Phys. Rev.* B **34** 5665